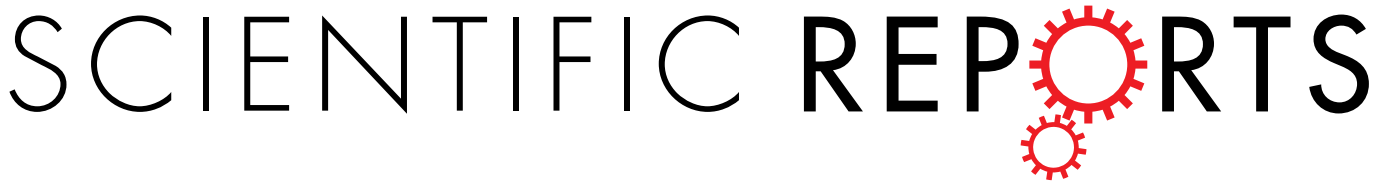

OPEN

The origin, type and hydrocarbon generation potential of organic matter in a marine-continental transitional facies shale succession (Qaidam Basin, China)

Received: 17 May 2017
Accepted: 13 April 2018
Published online: 26 April 2018

Guo-Cang Wang[1], Min-Zhuo Sun[1], Shu-Fang Gao[2] & Li Tang[2]

This organic-rich shale was analyzed to determine the type, origin, maturity and depositional environment of the organic matter and to evaluate the hydrocarbon generation potential of the shale. This study is based on geochemical (total carbon content, Rock-Eval pyrolysis and the molecular composition of hydrocarbons) and whole-rock petrographic (maceral composition) analyses. The petrographic analyses show that the shale penetrated by the Chaiye 2 well contains large amounts of vitrinite and sapropelinite and that the organic matter within these rocks is type III and highly mature. The geochemical analyses show that these rocks are characterized by high total organic carbon contents and that the organic matter is derived from a mix of terrestrial and marine sources and highly mature. These geochemical characteristics are consistent with the results of the petrographic analyses. The large amounts of organic matter in the Carboniferous shale succession penetrated by the Chaiye 2 well may be due to good preservation under hypersaline lacustrine and anoxic marine conditions. Consequently, the studied shale possesses very good hydrocarbon generation potential because of the presence of large amounts of highly mature type III organic matter.

Because of the successful commercial exploration and development of shale gas in the USA[1–3], large investments in the exploration and production of shale gas, an alternative hydrocarbon resource, have been made in China in recent years[4,5]. At the same time, studies have yielded many notable findings regarding depositional environments of marine or terrestrial shales, the formation conditions, accumulation mechanisms and enrichment patterns of shale gas, and the distribution of shale gas reservoirs[6–9]. However, to date, only a few geologists have investigated the geochemical and reservoir characteristics, gas-bearing conditions, shale gas accumulation conditions, and exploration prospects of transitional facies between marine and terrestrial environments[10,11]. The area investigated in this study is located in the Delingha depression of the Qaidam Basin in western China. Despite the relatively numerous oil exploration studies in this area[12–14], few studies on the organic geochemical characteristics or hydrocarbon generation potential of the marine-terrigenous facies shale have been published[15]. Cao (2016) simply analyzed the type, amount and maturity of the organic matter on the marine-terrigenous facies shale and mainly studied characteristics and factor of shale gas in this area[15], but origin of the organic matter and hydrocarbon generation potential were not reported. In this study, organic geochemical (especially biomarkers) and petrographic methods were used to examine the marine-terrigenous facies shale found in the Delingha depression of the Qaidam Basin. The objectives of this study were to determine the type, amount, origin and maturity of the organic matter found in these rocks as a function of their depositional environment and to evaluate their hydrocarbon generation potential. A series of analyses, including gas chromatography–mass spectrometry (GC-MS),

[1]Key Laboratory of Petroleum Resources, Gansu Province/Key Laboratory of Petroleum Resources Research, Institute of Geology and Geophysics/The Analytical Service center, Research Center of Oil and Gas Resources, Northwest Institute of Eco-environment and Resources, CAS, Lanzhou, 730000, PR China. [2]PetroChina Qinhai Oilfield Research Institute of Exploration & Development, Dunhuang, 736202, PR China. Shu-Fang Gao and Li Tang contributed equally to this work. Correspondence and requests for materials should be addressed to M.-Z.S. (email: sunmz04@sina.com)

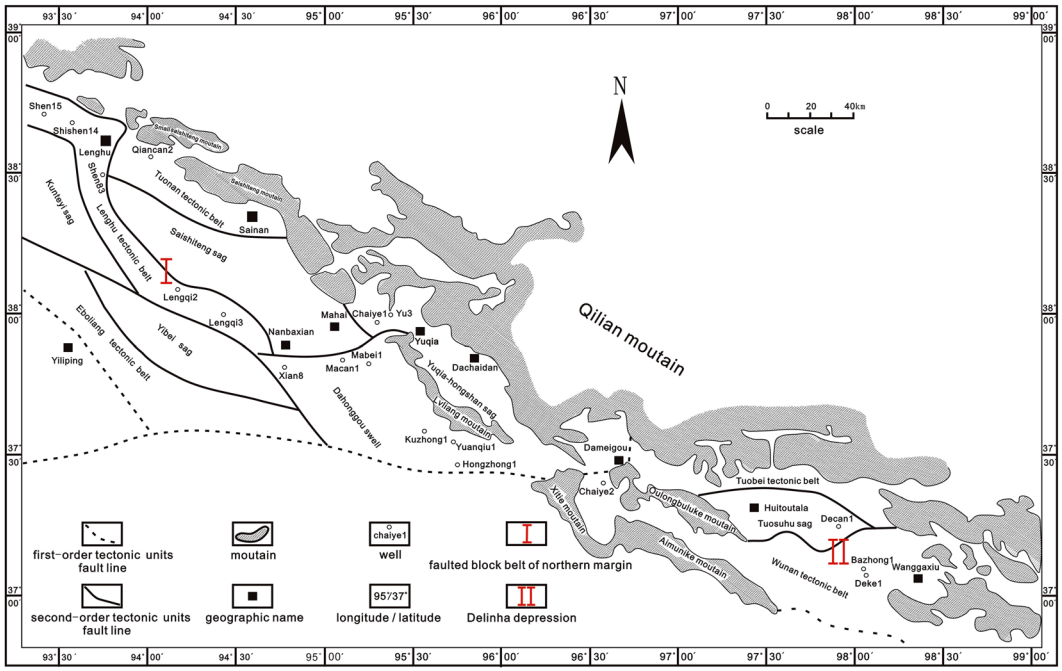

Figure 1. Tectonic units in the Qaidam Basin and the location of the Chaiye 2 well. The maps were created using CorelDRAWGraphicsSuite2017Installer_RW (http://www.coreldraw.com/cn/product/graphic-design-software/trial-thank-you.html?ver=18.0).

Rock-Eval pyrolysis, total organic carbon (TOC) evaluation, vitrinite reflectance assessment, and maceral group identification, were performed to meet these goals.

Geological Background

A total of 36 shale samples were collected from depths between 40 and 1050.8 meters in the Chaiye 2 well, which is located in the Qaidam Basin, China. The northern margin of the Qaidam Basin is one of the key onshore petroliferous blocks within the basin. It is composed of two first-order tectonic units and eleven second-order tectonic units. The first-order tectonic units are the faulted block of the northern margin and the Delingha depression. The faulted block of the northern margin includes eight tectonic subunits, namely, the Tuonan tectonic belt, the Saishiteng sag, the Yuqia-Hongshan sag, the Lenghu tectonic belt, the Yibei sag, the Kunteyi sag, the Eboliang tectonic belt and the Dahonggou swell. The Delingha depression can be divided into three subunits, specifically, the Tuobei tectonic belt, the Tuosuhu sag and the Wulan tectonic belt.

The Delingha depression covers an NW-SE-oriented area of approximately 1.8×104 km^2 and contains a Jurassic intracontinental rift basin superimposed on an early Paleozoic passive continental margin rift basin and a Neopaleozoic back-arc rift basin. The tectonic deformation within the Delingha depression is intense, and local structures are well developed. The development of the Delingha depression was strongly controlled by the tectonic evolution of the Xitie, Oulongbuluke, Aimunike and Qilian Shan orogenic belts; thus, the sag zone between the orogenic belts is the most favorable area for oil and gas exploration.

The sedimentary sequence within the Delingha depression is well developed and preserved, and it contains Cambrian marine carbonates, Ordovician marine carbonate-detrital rocks, Devonian green and purple detrital rocks, Carboniferous marine-continental transitional sedimentary rocks and Permian shallow-sea and deep-sea marine carbonate and detrital rocks. The Carboniferous strata are composed of the lower Carboniferous Chengqianggou (C1c) and Huitoutala (C1h) formations and the upper Carboniferous Keluke (C2k) and Zhabusagaxiu formations. These strata represent the marine-continental transitional sedimentary facies. The Chaiye 2 well is located within the Wulan tectonic belt and penetrates the upper Carboniferous Keluke formation. This unit is mainly composed of dark shale, mudstone, carbonaceous shale and coal[16,17] (Fig. 1).

Results

TOC and Rock-Eval pyrolysis. To investigate the origin, type and hydrocarbon generation potential of shale, we studied the characteristic of its insoluble organic matter by Rock-Eval to determine the Total Organic Carbon content(TOC), free hydrocarbons (S1), hydrocarbon generative potential (S2), temperature (Tmax) at themaximum of the S2 peak, and production index (PI = S1/(S1 + S2)), hydrogen index (HI = S2/TOC × 100). The Rock-Eval data and the PI and HI values of the samples are listed in Table 1. The TOC contents of the 36 shale samples ranged from 0.29% to 14.10%, and the average TOC content of all samples was 3.75%. The S1 values of the studied shale samples ranged from 0.03 mg HC/g to 1.84 mg HC/g, and the S2 values ranged from 0.14 mg HC/g to 13.46 mg HC/g. The Tmax values of the shale samples ranged from 443 °C to 460 °C, with an average value of 452 °C. The HI values of the shale samples ranged from 10.28 mg HC/g TOC to 102.51 mg HC/g TOC,

Sample	Depth (m)	Lithology	TOC (wt %)	Rock-Eval pyrolysis				
				S1 (mg HC/g)	S2 (mg HC/g)	Tmax (°C)	HI (mg HC/g TOC)	PI
CY1	40	black mudstone	3.77	0.17	0.82	445	21.75	0.17
CY2	100	ashen mudstone	0.71	0.03	0.17	445	23.94	0.15
CY3	150	black mudstone	3.79	0.17	0.76	451	20.05	0.18
CY4	245	black shale	3.83	0.34	3.07	447	80.16	0.10
CY5	332	black shale	2.97	0.07	0.43	444	14.48	0.14
CY6	395	gray-black shale	1.50	0.05	0.21	443	14.00	0.19
CY7	476	black shale	2.06	0.31	0.99	455	48.06	0.24
CY8	514	black carbonaceous shale	7.27	0.21	0.82	445	11.28	0.20
CY9	603	black coal	13.13	1.84	13.46	452	102.51	0.12
CY10	653.63	gray shale	0.72	0.10	0.25	460	34.72	0.29
CY11	654.03	gray shale	0.30	0.03	0.14	443	46.67	0.18
CY12	654.75	black shale	3.39	0.33	0.76	460	22.42	0.30
CY13	655.42	gray shale	0.29	0.08	0.16	460	55.17	0.33
CY14	657.03	black shale	2.67	0.13	0.30	456	11.24	0.30
CY15	657.43	black shale	2.53	0.62	1.39	447	54.94	0.31
CY16	660.73	black carbonaceous shale	6.94	0.70	3.66	455	52.74	0.16
CY17	661.28	black coal	14.10	1.29	11.60	452	82.27	0.10
CY18	840.6	black shale	2.43	0.14	0.44	457	18.11	0.24
CY19	846.1	black shale	2.72	0.15	0.66	448	24.26	0.19
CY20	902.56	gray-black shale	1.18	0.07	0.26	446	22.03	0.21
CY21	911.37	gray-black shale	1.69	0.09	0.35	445	20.71	0.20
CY22	918.07	black carbonaceous shale	8.51	0.50	3.70	448	43.48	0.12
CY23	920.39	black shale	2.06	0.06	0.33	462	16.02	0.15
CY24	933.94	gray-black shale	3.74	0.10	0.43	446	11.50	0.19
CY25	938	black shale	2.53	0.14	0.94	448	37.15	0.13
CY26	954.1	black shale	2.14	0.03	0.22	458	10.28	0.12
CY27	970.3	gray shale	0.89	0.04	0.2	453	22.47	0.17
CY28	988.05	black shale	2.83	0.14	0.74	454	26.15	0.16
CY29	994.15	black limestone	2.31	0.12	0.54	456	23.38	0.18
CY30	997.15	black shale	4.49	0.19	1.19	455	26.50	0.14
CY31	999.2	black shale	2.32	0.12	0.72	458	31.03	0.14
CY32	1019.3	black shale	2.18	0.03	0.23	459	10.55	0.12
CY33	1035.1	black carbonaceous shale	9.28	0.43	3.44	459	37.07	0.11
CY34	1035.3	black shale	3.40	0.14	0.60	451	17.65	0.19
CY35	1048.7	black carbonaceous shale	8.72	0.37	3.79	458	43.46	0.09
CY36	1050.8	gray-black shale	1.54	0.07	0.44	466	28.57	0.14

Table 1. Main geochemical characteristics of pyrolysis study on shale samples, as determined by Rock-Eval analysis. Total Organic Carbon (TOC) is given in percent. S1 represents free hydrocarbons, S2 represents the hydrocarbon generative potential, Tmax represents the temperature at themaximum of the S2 peak. Production index (PI = S1/[S1 + S2]) and hydrogen index (HI = S2/TOC × 100).

with an average value of 32.41 mg HC/g TOC. The PI values of the shale samples ranged from 0.09 to 0.32, with an average value of 0.18.

Vitrinite reflectance and maceral groups. The vitrinite reflectance values (Ro, %) of the samples range from 1.09–1.53%. The Ro values of 80% of the samples fell within the range of 1.3–2.0%, and the Ro values of 20% of the samples fell within the range of 0.7–1.3% (Table 2).

The maceral contents of the shale samples are shown in Table 2 and in selected photomicrographs (Fig. 2). The shale samples contain high vitrinite contents (mean content of 64.22%) and trace amounts of exinite. These samples also contain abundant sapropelinite (20.73–42.87%) and small amounts of inertinite (mean content of 1.15%) (Table 2, Fig. 2). Telocollinite was the most common form of vitrinite (Fig. 3a), and the inertinite was mainly composed of fusinite (Fig. 3b). Mineralized bituminous groundmass was the main form of sapropelinite (Fig. 3c), and organic inclusions were identified in some samples (Fig. 3d).

Molecular composition of hydrocarbons

***n*-Alkanes and isoprenoid hydrocarbons.** The *n*-alkanes and isoprenoid hydrocarbons were distributed differently in samples obtained from different depths (Fig. 4, CY3(150 m)-m/z 85). The samples obtained

Sample	Depth (m)	Lithology	Ro (%)	a (%)	b (%)	c (%)	d (%)	KTI	Organic matter type
CY4	245	black shale	1.09	41.68	Trace	57.82	0.5	−2.2	III
CY7	476	black shale	1.20	39.06	Trace	60.12	0.82	−6.9	III
CY9	603	black coal	1.17	34.49	Trace	64.31	1.2	−14.9	III
CY13	655.42	gray shale	1.30	31.12	Trace	67.98	0.9	−20.8	III
CY17	661.28	black coal	1.19	21.21	Trace	76.84	1.95	−38.4	III
CY18	840.6	black shale	1.38	22.26	Trace	76.14	1.6	−36.4	III
CY20	902.56	gray-black shale	1.49	36.18	Trace	62.72	1.1	−12.0	III
CY21	911.37	gray-black shale	1.46	40.15	Trace	59.29	0.56	−4.9	III
CY22	918.07	black carbonaceous shale	1.37	38.64	Trace	60.96	0.4	−7.5	III
CY24	933.94	gray-black shale	1.46	40.83	Trace	58.27	0.9	−3.8	III
CY25	938	black shale	1.43	29.19	Trace	69.01	1.8	−24.4	III
CY26	954.1	black shale	1.46	20.73	Trace	77.23	2.04	−39.2	III
CY27	970.3	gray shale	1.44	41.46	Trace	57.94	0.6	−2.6	III
CY28	988.05	black shale	1.50	34.45	Trace	64.55	1	−15.0	III
CY31	999.2	black shale	1.39	35.63	Trace	62.97	1.4	−13.0	III
CY32	1019.3	black shale	1.53	39.73	Trace	59.97	0.3	−5.5	III
CY33	1035.1	black carbonaceous shale	1.52	42.87	Trace	56.16	0.97	−0.2	III
CY34	1035.3	black shale	1.48	34.86	Trace	63.04	2.1	−14.5	III
CY35	1048.7	black carbonaceous shale	1.46	38.35	Trace	60.85	0.8	−8.1	III
CY36	1050.8	gray-black shale	1.46	29.72	Trace	68.18	2.1	−23.5	III

Table 2. Maceral groups, the vitrinite reflectance values (Ro) and proximate analysis of the studied shale samples. a (%), b (%), c (%) and d (%) represent the volume percentages of sapropelinite, exinite, vitrinite and inertinite in shale maceral groups, respectively. Kerogen type index (KTI) = (100 × a + 50 × b − 75 × c − 100 × d)/100. The organic matter is predominantly type III (KTI < 0), the organic matter is predominantly type II2 (0 ≤ KTI < 40), the organic matter is predominantly type II1(40 ≤ KTI < 80), the organic matter is predominantly type I (KTI ≥ 80).

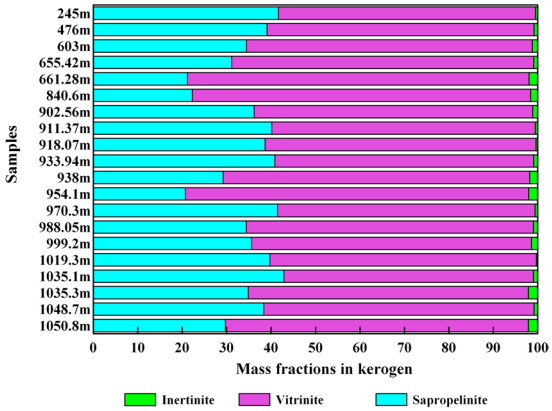

Figure 2. Bar plot of maceral composition showing the mass fractions of inertinite, vitrinite, exinite, and sapropelinite for all shale samples obtained from the Chaiye 2 well.

from 40 to 661.28 meters contained *n*-alkanes ranging from *n* -C_{12} to *n*-C_{34}. The *n* -alkane distributions were unimodal in these samples, and the samples display a consistent maximum at *n*-C_{17}. The ranges of *n*-alkanes differ between the samples obtained from depths of 40 to 661.28 meters and those from 840.6 to 1050.8 meters (Fig. 4, CY18(840.6 m)-m/z 85). The *n* -alkane distribution pattern observed in the samples obtained from 840.6 to 1050.8 meters reflected abundant *n* -C_{14} to *n* -C_{33}. Moreover, this pattern displayed a bimodal distribution with a consistent maximum at *n* -C_{25} and prominence at *n* -C_{18}.

The studied samples had carbon preference index (CPI) values that range from 0.97 to 1.13 (Table 3). The $\sum nC_{21}^{-}/\sum nC_{22}^{+}$ ratios of the shale samples obtained from depths between 40 and 661.28 meters and 840.6 and 1050.8 meter ranged from 1.60 to 9.43 and 0.42 to 1.78, respectively (Table 3).

Isoprenoid hydrocarbons were abundant in all of the shale samples and were represented by pristane (Pr) and phytane (Ph) (Fig. 4). The Pr/Ph ratios of the samples obtained from depths between 40 and 661.28 meters and 840.6 and 1050.8 meters range from 0.72 to 1.85 and 0.85 to 1.48, respectively (Table 3). The Pr/n-C_{17} and Ph/n-C_{18} values were very low and ranged from 0.08 to 0.70 and 0.06 to 0.84, respectively (Table 3).

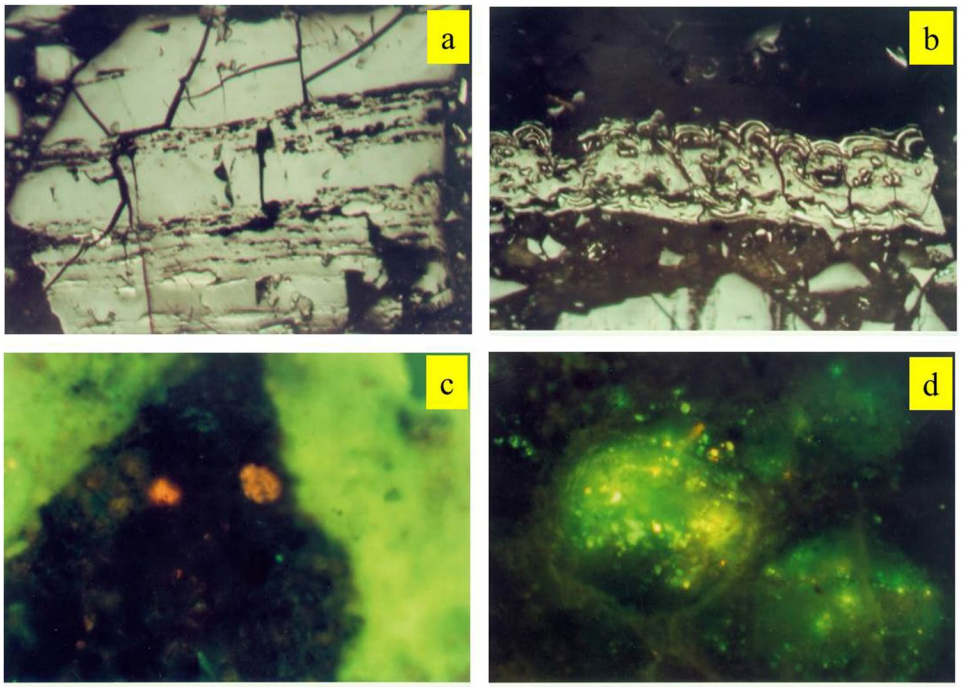

Figure 3. Photomicrographs of telocollinite (**a**), fusinite (**b**), mineral bituminous groundmass (**c**), and organic inclusions (**d**) observed in shale samples obtained from the Chaiye 2 well located in the Qaidam Basin under reflected light (**a**,**b**) and transmitted light (**c**,**d**) (field width = 0.2 mm).

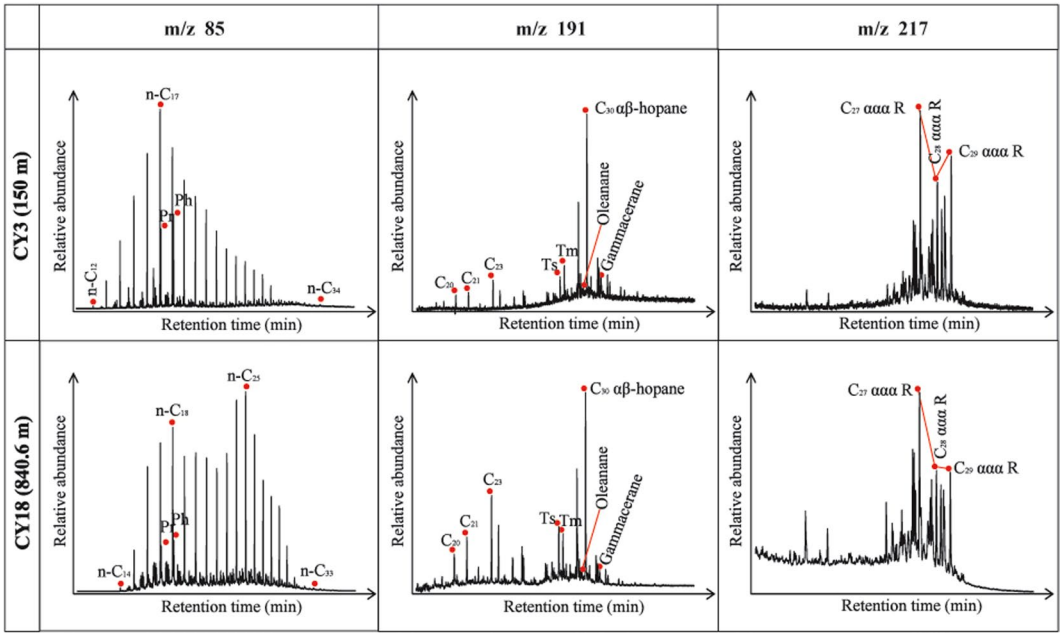

Figure 4. Ion chromatograms of m/z 85 (*n*-alkanes and isoprenoid hydrocarbons), 191 (tricyclic to pentacyclic terpanes) and 217 (steranes) for saturate hydrocarbon (saturate hydrocarbon were separated from by column chromatography). Within depth range of 40 to 661.28 meters, the CY3(150 m) is representative of all samples. Within dep th range of 840.6 to 1050.8 meters, the CY18(840.6 m) is representative of all samples.

Tricyclic to pentacyclic terpanes. The tricyclic to pentacyclic terpanes identified by m/z 191 are shown in Fig. 4 -m/z 191. Additionally, the key parameters calculated for these tricyclic to pentacyclic terpanes are displayed in Table 3.

Sample	Pr/Ph	Pr/ n-C_{17}	Ph/ n-C_{18}	CPI	A	B	C_{27}(%)	C_{28}(%)	C_{29}(%)	C	D	E	F	G	H	DBT/P	MPI	Rc(%)
CY1	0.78	0.58	0.77	1.02	1.64	1.36	33.26	27.40	39.34	0.43	0.47	0.08	0.01	0.58	0.45	0.19	0.67	1.04
CY2	0.87	0.70	0.84	1.05	2.23	1.41	32.21	24.83	42.96	0.41	0.44	0.08	0.02	0.60	0.51	0.19	0.61	1.00
CY3	0.85	0.39	0.58	1.08	4.83	1.02	41.84	26.36	31.80	0.39	0.42	0.11	0.03	0.57	0.42	0.23	0.81	1.12
CY4	1.04	0.42	0.44	1.04	4.11	0.98	41.17	26.38	32.45	0.35	0.40	0.08	0.02	0.59	0.47	0.16	0.85	1.15
CY5	0.72	0.59	0.77	1.00	5.38	1.37	32.89	25.97	41.14	0.39	0.44	0.08	0.02	0.56	0.50	0.18	0.82	1.13
CY6	0.85	0.52	0.68	1.05	5.19	1.30	34.22	26.72	39.06	0.43	0.45	0.08	0.02	0.57	0.49	0.12	0.93	1.20
CY7	0.85	0.52	0.68	1.05	5.19	1.13	36.57	25.07	38.35	0.48	0.56	0.10	0.08	0.59	0.56	0.11	0.97	1.22
CY8	0.93	0.29	0.34	1.13	2.49	1.25	34.89	27.20	37.91	0.43	0.51	0.10	0.05	0.61	0.49	0.09	0.94	1.20
CY9	1.01	0.43	0.47	0.99	5.01	0.87	44.30	22.88	32.82	0.46	0.45	0.11	0.05	0.61	0.45	0.16	1.04	1.26
CY10	1.63	0.47	0.30	1.01	2.10	0.84	44.85	24.83	30.32	0.46	0.48	0.11	0.03	0.54	0.59	0.14	1.10	1.30
CY11	1.1	0.20	0.19	1.03	4.89	0.91	44.29	22.76	32.95	0.47	0.45	0.11	0.03	0.60	0.57	0.12	1.10	1.30
CY12	1.85	0.44	0.20	1.02	1.60	0.89	43.00	22.61	34.38	0.46	0.49	0.09	0.04	0.59	0.57	0.16	1.04	1.26
CY13	1.34	0.50	0.39	1.00	1.81	0.97	42.93	25.51	31.56	0.46	0.47	0.11	0.04	0.61	0.55	0.17	1.06	1.27
CY14	1.59	0.27	0.19	1.01	3.38	1.02	40.08	23.71	36.20	0.42	0.42	0.12	0.03	0.58	0.53	0.12	1.17	1.34
CY15	1.36	0.08	0.06	1.03	3.17	1.00	38.35	26.48	35.17	0.43	0.48	0.11	0.05	0.52	0.51	0.14	1.16	1.34
CY16	1.19	0.09	0.10	1.09	9.43	1.05	37.62	26.40	35.98	0.43	0.46	0.11	0.04	0.51	0.47	0.56	1.19	1.35
CY17	1.48	0.35	0.25	1.01	1.86	1.14	36.78	27.03	36.19	0.49	0.50	0.11	0.04	0.56	0.50	0.11	1.21	1.37
CY18	1.48	0.35	0.38	1.01	1.01	0.70	46.90	25.95	27.15	0.45	0.43	0.07	0.07	0.59	0.54	0.28	1.24	1.39
CY19	1.4	0.38	0.35	1.03	1.07	0.71	47.30	24.74	27.97	0.51	0.42	0.10	0.07	0.59	0.57	0.09	1.40	1.48
CY20	1.35	0.28	0.32	1.06	0.42	0.62	48.07	27.12	24.81	0.45	0.38	0.09	0.03	0.58	0.55	0.07	1.19	1.35
CY21	1.27	0.33	0.37	1.00	0.75	0.94	43.14	25.39	31.48	0.48	0.44	0.09	0.02	0.60	0.55	0.07	1.26	1.40
CY22	1.05	0.29	0.34	1.04	1.78	0.94	41.98	26.74	31.28	0.38	0.39	0.09	0.04	0.58	0.56	0.12	1.31	1.43
CY23	0.85	0.32	0.39	0.97	0.90	0.84	43.00	24.43	32.57	0.47	0.42	0.11	0.04	0.58	0.55	0.09	1.28	1.41
CY24	0.94	0.38	0.44	1.03	0.89	0.63	50.98	24.98	24.04	0.46	0.41	0.09	0.05	0.61	0.62	0.09	1.18	1.35
CY25	1.15	0.35	0.36	0.97	1.26	0.65	46.83	27.09	26.08	0.50	0.43	0.09	0.02	0.58	0.54	0.10	1.36	1.46
CY26	1.09	0.34	0.45	1.08	0.51	0.72	47.21	25.92	26.87	0.47	0.40	0.07	0.03	0.59	0.54	0.11	1.18	1.35
CY27	1.08	0.41	0.44	0.99	0.72	0.89	42.41	26.82	30.77	0.42	0.39	0.12	0.04	0.58	0.51	0.10	1.09	1.29
CY28	1.01	0.40	0.48	0.99	1.37	0.77	45.80	25.04	29.15	0.50	0.41	0.08	0.05	0.59	0.53	0.13	1.28	1.41
CY29	1.14	0.44	0.45	1.04	0.93	0.73	48.49	24.93	26.59	0.44	0.39	0.10	0.11	0.58	0.62	0.14	1.11	1.31
CY30	1.14	0.36	0.39	1.04	1.11	0.68	47.92	25.22	26.87	0.45	0.40	0.10	0.03	0.58	0.61	0.14	1.42	1.49
CY31	0.97	0.35	0.44	1.06	1.01	0.61	52.47	24.02	23.51	0.45	0.40	0.10	0.04	0.56	0.63	0.12	1.27	1.40
CY32	1.06	0.40	0.52	1.06	1.32	0.73	47.91	24.95	27.15	0.47	0.40	0.08	0.04	0.57	0.57	0.09	1.17	1.34
CY33	1.23	0.40	0.47	1.04	1.70	0.82	45.11	26.06	28.83	0.47	0.41	0.11	0.03	0.59	0.58	0.17	1.34	1.45
CY34	1.19	0.39	0.44	1.02	1.05	0.79	46.99	23.92	29.09	0.52	0.43	0.10	0.04	0.56	0.53	0.12	1.19	1.36
CY35	1.14	0.33	0.43	1.06	0.82	0.83	44.63	25.00	30.37	0.43	0.39	0.11	0.03	0.58	0.60	0.15	1.23	1.38
CY36	0.94	0.34	0.43	1.07	0.95	0.90	42.18	26.22	31.60	0.43	0.39	0.11	0.04	0.58	0.60	0.10	1.21	1.37

Table 3. Molecular marker parameters and biomarker indexes for extracts from shale samples obtained from the Chaiye 2 well located in the Qaidam Basin. Pr, Ph, *n*-C_{17}, *n*-C_{18}, Ts, Tm, DBT, P,MPI, MP and Rc represent pristine, phytane, *n*-heptadecane, *n*-octadecane, 18α (H) −22, 29, 30-trinorhopane, 17α (H) −22, 29, 30-trinorhopane, dibenzothiophene, phenanthrene, methylphenanthrene index, methylphenanthrene (MPI = 1.5(3-MP + 2-MP)/(P + 9-MP + l-MP)), equivalent vitrinite reflectance (Rc = 0.6MPI + 0.64), respectively. Carbon preference index (CPI) = $(C_{17}+C_{19}+C_{21}+C_{23}+C_{25})/(C_{16}+C_{18}+C_{20}+C_{22}+C_{24})/2 + (C_{17}+C_{19}+C_{21}+C_{23}+C_{25})/(C_{18}+C_{20}+C_{22}+C_{24}+C_{26})/2$. A represents the ratio of lower molecular weight ($\leq C_{21}$) *n*-alkanes ($\sum nC_{21}^{-}$) to higher molecular weight ($\geq C_{22}$) *n*-alkanes ($\sum nC_{22}^{+}$), B represents the ratio of C_{29} regular steranes to C_{27} regular steranes. C_{27}(%), C_{28}(%) and C_{29}(%) represent the ratio of C_{27}αα-20R, C_{28}αα-20R and C_{29}αα-20R to the total of C_{27}, C_{28} and C_{29}αα 20R sterane. C, D, E, F, and G represent the parameter of sterane C_{29}αα-20S/(20S+20R), the parameter of sterane C_{29}-ββ/(ββ+αα), gammacerane index(gammacerane/C_{30} αβhopane), oleanane index(oleanane/C_{30} αβ hopane), the parameter of hopane C_{31}-22S/(22S + 22R), respectively. H represents the ratio of Ts to total of Ts and Tm.

Tricyclic terpanes C_{19} to C_{29} were identified in the shale samples. The content of C_{22} and C_{27} were very low. The most prominent peak in the tricyclic terpanes series was that of C_{23}, as shown in Fig. 4 -m/z 191. The tricyclic terpanes C_{26} to C_{29} were characterized by doublets in the Ion chromatograms, and the doublets contained S and R isomers. Moreover, pentacyclic terpanes from C_{27} to C_{35} were present. Of these, C_{30} (hopane) had the highest relative abundance, whereas the abundance of C_{28} was unusually low. Trisnorhopane (C_{27}) and homohopanes (C_{31}^{+}) appeared as doublets (18α(H)and 17α(H); 22S and 22R epimers, respectively) in the Ion chromatograms

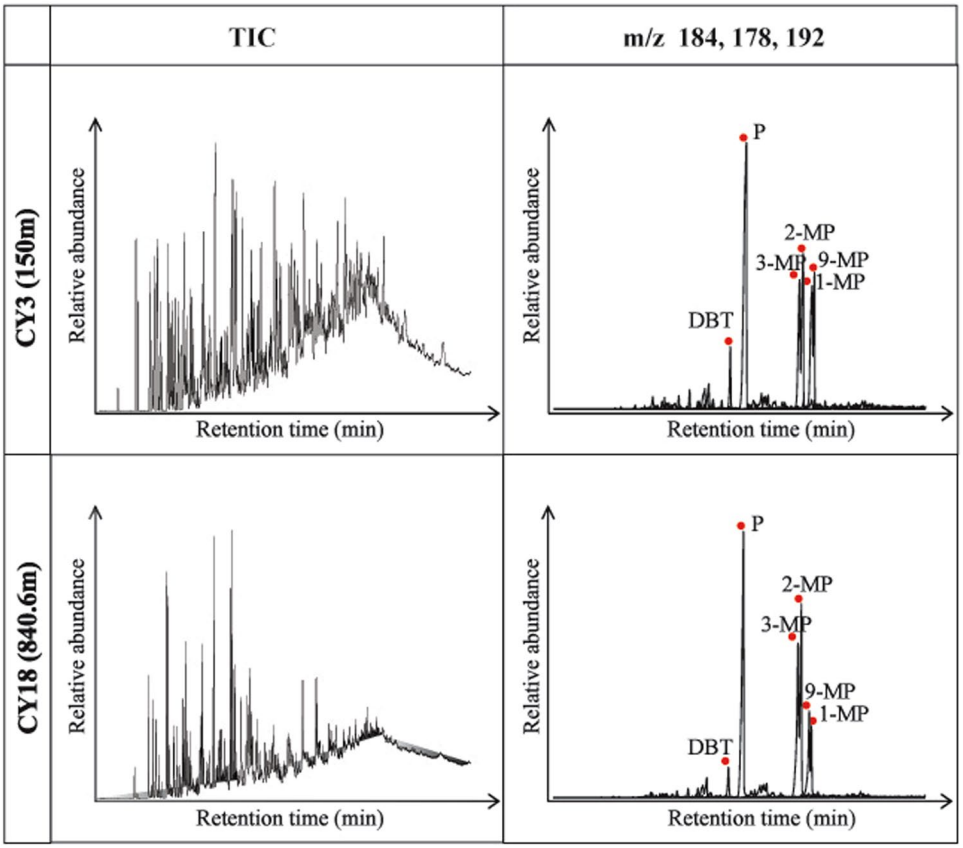

Figure 5. Gas chromatograms (TIC) and ion chromatograms of m/z 184 (dibenzothiophene), 178 (phenanthrene) and 192 (methylphenanthrenes) for aromatics of extracts from the studied samples. Within depth range of 40 to 661.28 meters, the CY3(150 m) is representative of all samples. Within depth range of 840.6 to 1050.8 meters, the CY18(840.6 m) is representative of all samples.

for all of the studied shale samples (Fig. 4 -m/z191). Oleanane and gammacerane also appearen in the Ion chromatograms (Fig. 4 -m/z191).

The gammacerane index (gammacerane/$C_{30}\alpha\beta$hopane) values of the studied shale samples range from 0.07–0.12 (Table 3). The oleanane index (oleanane/$C_{30}\alpha\beta$hopane) values of these samples ranged from 0.01–0.11 (Table 3). The doublets of trisnorhopane (C_{27}) contained 18α (H)-trisnorhopane (Ts) and 17α (H)-trisnorhopane (Tm) isomers. For these samples, the maturity index C_{31}22S/(22S + 22R) and Ts/(Ts + Tm) values of the pentacyclic terpane series ranged from 0.51 to 0.61 and 0.42to 0.63, respectively (Table 3).

Steranes. The mass chromatograms of m/z 217of the studied shale samples reflect enrichments in the 14α(H) and 17α(H) structural isomers, with a predominance of C_{27} or C_{29} relative to C_{28} regular steranes and diasteranes (C_{27}–C_{29}) and low abundances of short-chain pregnanes (C_{20} and C_{21}) (Fig. 4 -m/z217).

For the studied shale samples, the ratios of C_{29} to C_{27} regular steranes (C_{29}/C_{27} regular steranes) ranged from 0.61–1.41, with an average value of 0.92. The maturity indexes of the steranes were $C_{29}\alpha\alpha$20S/(20S + 20R) and $C_{29}\beta\beta/(\beta\beta + \alpha\alpha)$, and the values of these indexes range from 0.35–0.52 and 0.38–0.56, respectively. Additionally, the percentage of the steranes $C_{27}\alpha\alpha$20R, $C_{28}\alpha\alpha$20R and $C_{29}\alpha\alpha$20R ranged from 32.21–52.47%, 22.61–27.40%, and 23.51–42.96%, respectively (Table 3).

Aromatics. The total ion chromatograms (TIC) of the aromatic fractions of the studied shale samples are shown in Fig. 5. The major aromatics were naphthalene series compounds (methyl-, dimethyl-, and trimethylnaphthalenes), phenanthrene series compounds (methyl-, dimethyl-, and trimethylphenanthrenes), biphenyl series compounds (methyl- and dimethylbiphenyl), fluorene, dibenzofuran series compounds (methyl- and dimethyldibenzofuran), dibenzothiophene and methyldibenzothiophene, chrysene and methylchrysene, fluoranthene and pyrene series compounds (methyl- and dimethylfluoranthene and pyrene), perylene, and benzofluoranthene and benzopyrene, which were dominated by phenanthrene and methylphenanthrenes.

The methylphenanthrene index (MPI), which is based on phenanthrene and methylphenanthrenes (3-, 2-, 9-, and 1-) (Fig. 5 -m/z 184, 178, 192), was calculated as a maturation parameter[18]. The MPI values of the studied shale samples range from 0.61 to 1.42. The equivalent vitrinite reflectance (Rc), which is based on an empirical relationship between the MPI and vitrinite reflectance, was used to assess maturity[18]. The Rc (%) values of the studied shale samples range from 1.00% to 1.49% (Table 3).

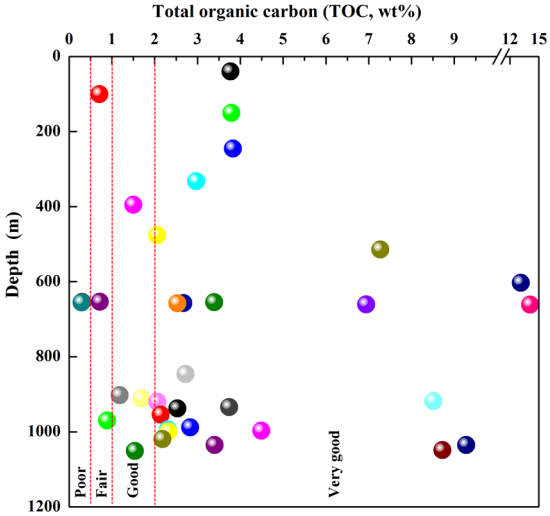

Figure 6. Distribution of total organic carbon (TOC, wt%) versus depth (m) for the shale samples obtained from the Chaiye 2 well.

The ratio of dibenzothiophene to phenanthrene (DBT/P) is thought to be an indicator of the depositional environment, origin and source rock lithology[19]. The values of the DBT/P ratio range from 0.07 to 0.56 (Table 3).

Discussion

Kerogen microscopy characteristics. The kerogen assemblage was recognized as dispersed organic matter, which includes phytoclasts (such as structureless amorphous organic matter, plant fragments, and marine-derived organic matter)[20]. The observation of kerogen with incident light and reflected light microscopy indicates that the organic matter found within the shale from the Chaiye 2 well is type III kerogen that contains a moderate amount of sapropelinite, traces of exinite, a high abundance of vitrinite and a low content of inertinite (Fig. 2, Table 2). The type of kerogen present can be described by the kerogen type index (KTI), which is calculated from the mass fractions of the different components of the kerogen[21]. According to the calculated results, the KTI values of all of the shale samples from the Chaiye 2 well were less than zero, reflecting type III kerogen[21] (Table 2).

Total organic carbon and types of organic matter. TOC (wt%) was used to determine the abundance of organic matter and to evaluate the hydrocarbon generation potential of the samples[22]. Based on the TOC contents, 75% of the samples can be classified as "very good" source rock quality (>2.0%), 11% of the samples had "good" source rock quality (1.0–2.0%), and 8% of the samples had "poor to fair" source rock quality (0.5–1.0%). Only two samples (CY11 and CY13) displayed "poor" quality (<0.5%)[23] (Table 1, Fig. 6).

The shale samples obtained from the Chaiye 2 well had low HI values (Table 1). That range of Tmax values may have resulted from the low HI values, as the organic matter was predominantly type III (Fig. 7). The organic matter types of determined using Rock-Eval pyrolysis were consistent with the microscopic observations.

Sources of the hydrocarbons. The *n*-alkanes in shale from the Chaiye 2 well exhibit different distributions and compositional characteristics (Fig. 4 -m/z85), leading to change of some parameters. The studied samples had high $\sum nC_{21}^{-}/\sum nC_{22}^{+}$ values from 40 to 661.28 meters, with a low $\sum nC_{21}^{-}/\sum nC_{22}^{+}$ values from 840.6 to 1050.8 meters (Table 3, Fig. 8). These data suggest that the organic matter in the shale at depths of 40 to 661.28 meters was derived from aquatic organisms[24] and at depths of 840.6 to 1050.8 meters was associated with a combination of aquatic organism and land plant sources[25].

The relative amounts of C_{27}–C_{29} αα 20R steranes can be used to indicate differences in the sources of organic matter[26], because C_{29} and C_{27} sterols are derived primarily from terrestrial plants and zooplankton, respectively[27]. The contents of C_{27} ααα 20R steranes in the shale samples obtained from the Chaiye 2 well were similar to or slightly higher than the contents of C_{29} αα 20R steranes (Fig. 9), indicating that the shale is associated with a mix of terrestrial and marine organic sources[28].

Depositional environments. The depositional environment of the studied samples was extrapolated from the pristane/phytane (Pr/Ph), Pr/n-C_{17}, Ph/n-C_{18}, C_{27}, C_{28} and C_{29} αα steranes, gammacerane and oleanane biomarker indexes.

The distributions of C_{27}, C_{28} and C_{29} αα 20R steranes can be used to determine the depositional environments of shales[29]. Notably, the steranes of all of the samples plot in the estuarine/bay portion of the ternary diagram (Fig. 9).

The Pr/Ph ratio generally indicates the redox conditions of the depositional environment and varies with water depth and input type. Low Pr/Ph values reflect suboxic environments, deep water and marine inputs[19,30]. The Pr/Ph values of the samples found at depths of 40–661.28 meters in the Chaiye 2 well tended to increase with increasing sample depth (Fig. 10). By contrast, the Pr/Ph values in samples found at depths of 840.6–1050.80 meters tended to decrease with increasing sample depth (Fig. 10). Thus, the depositional environment of the studied

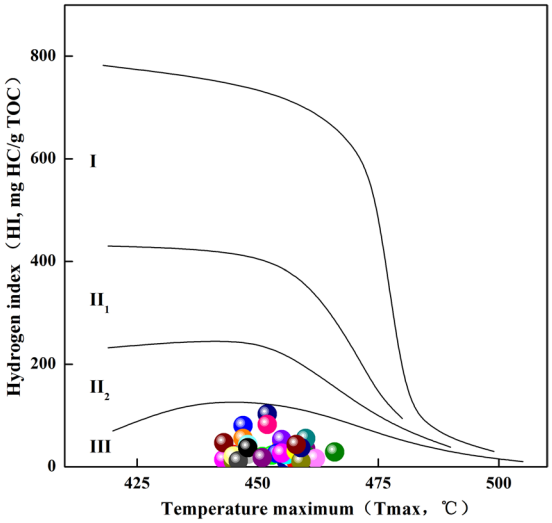

Figure 7. Plot of hydrogen index (HI) versus Tmax showing the kerogen types of the shale samples obtained from the Chaiye 2 well.

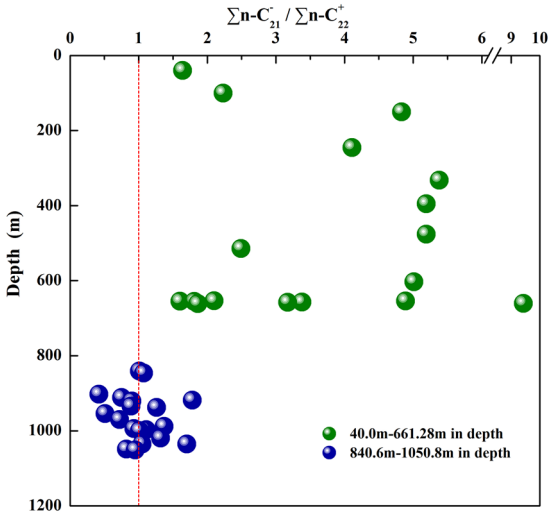

Figure 8. Distribution of n-C_{21}^{-}/n-C_{22}^{+} versus depth for the shale samples obtained from the Chaiye 2 well.

samples transitioned from deep to shallow to deep, which is typical of sediments found in marine-continental transitional sedimentary facies. The relationship between the isoprenoid Pr/n-C_{17} and Ph/n-C_{18} ratios in the studied shale supports this interpretation and indicates a weakly oxic to weakly reducing pattern characteristic of sediments deposited in alternating sea and riverine facies[29] (Fig. 11). This conclusion is also supported by the plot of the Pr/Ph ratio versus the C_{29}/C_{27} regular sterane ratio[31] (Fig. 12).

Gammacerane is an important C_{30} triterpane and may originate from tetrahymanols, which are widespread in marine sediments[32,33]. High gammacerane contents are typical of high-salinity environments and commonly result from hypersalinity and suboxidation at depth[34]. Therefore, gammacerane content can be used to identify the existence of stratified water columns in the depositional environments of marine and non-marine source rocks[35]. The shale samples obtained from the Chaiye 2 well had low the gammacerane index (gammacerane/$\alpha\beta C_{30}$ hopane) values. This range suggests weakly reducing, brackish conditions during the deposition of the source rocks[36]. The ratio of dibenzothiophene to phenanthrene (DBT/P) is thought to be an indicator of depositional environment, organic matter source and the source rock lithology[19]. The DBT/P values of samples from the Chaiye 2 well decreased with depth (Table 3). A plot of the DBT/P and Pr/Ph ratios (Fig. 13) shows that the samples obtained from the Chaiye 2 well fell on the boundary between marine and lacustrine shales and hypersaline lacustrine and anoxic marine deposits.

Oleanane, a biomarker indicative of higher terrigenous plants, has been suggested as an indicator of angiosperms (flowering plants)[37]. The ratio of oleanane to C_{30} hopane (deemed the oleanane index) provides information regarding depositional environments and source rock ages[38]. Oleanane index value greater than 0.2 indicate

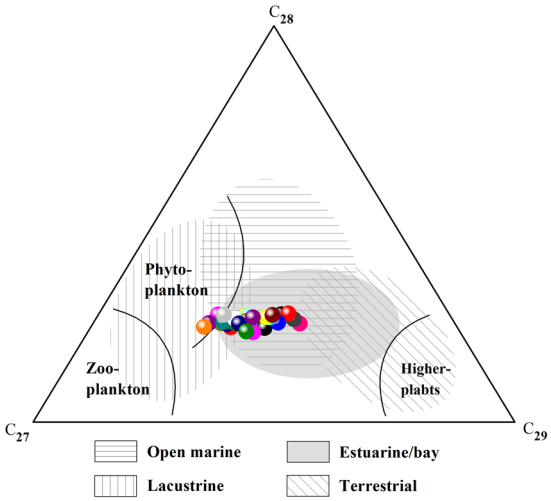

Figure 9. Ternary plot showing the relative contents of C_{27}, C_{28} and C_{29} αα 20R steranes. Paleoenvironmental and source interpretations based on Armelle *et al.*[29].

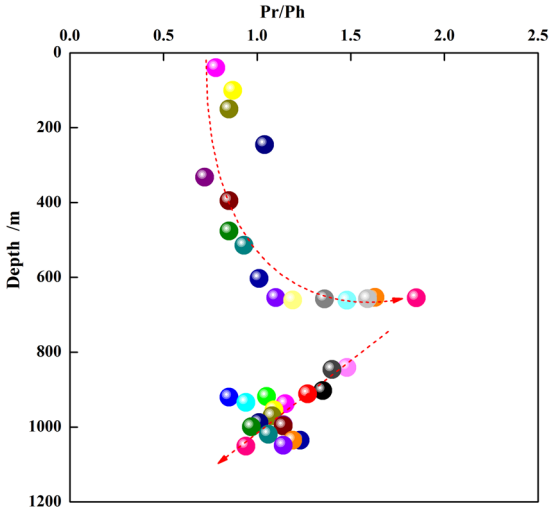

Figure 10. Ratio of pristane to phytane with depth in shale samples obtained from the Chaiye 2 well.

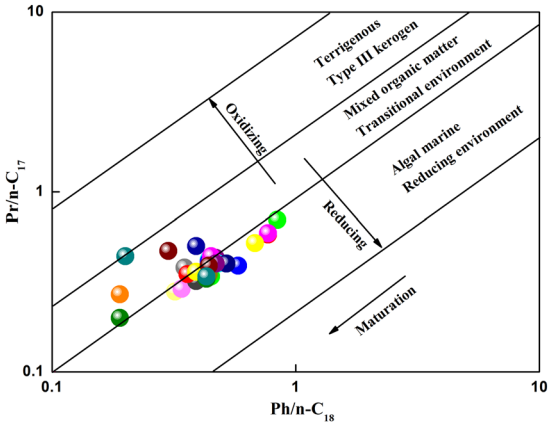

Figure 11. Plot of Pr/n-C17 versus Ph/n-C18 for shale samples obtained from the Chaiye 2 well. (interpretive scheme from Armelle *et al.*[29]).

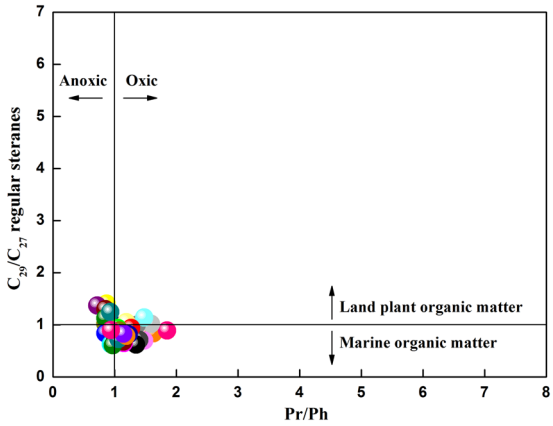

Figure 12. Depositional environment and organic matter input of the shale samples obtained from the Chaiye 2 well, as inferred from the ratio of Pr/Ph versus the ratio of regular sterane C_{29}/C_{27}.

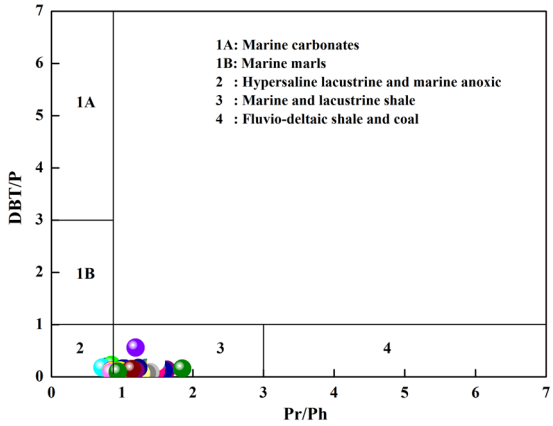

Figure 13. Ratio of dibenzothiophene to phenanthrene (DBT/P) plotted against the ratios of pristane to phytane (Pr/Ph) to determine shale depositional environments.

that the sample was deposited during the Tertiary and in a marine deltaic environment[19]. By contrast, oleanane index values less than 0.2 are characteristic of Cretaceous source rocks deposited in marine deltaic or marine shelf environments[19]. Figure 14 can be used to assess the depositional environment of the shale samples based on the Pr/Ph ratios and oleanane index values. The figure suggests that the studied shale samples are likely associated with a marine shelf depositional environment.

Maturity. The maturities of the samples obtained from the Chaiye 2 well in the Qaidam Basin were studied using the Ro and Tmax values and several biomarker parameters.

The Ro (%) values of the samples were grester than 0.7% (Table 2), indicating a high degree of maturity. Based on the Ro values, 80% of the samples can be characterized as highly mature (1.3–2.0%), and 20% of the samples can be characterized as mature (0.7–1.3%)[18] (Table 2).

The Tmax values of the samples were greater than 440 °C (Table 1), indicating mature to highly mature stages[39].

The CPI values of the n-alkanes[30], the sterane isomerization parameters $C_{29}\alpha\alpha 20S/(20S+20R)$ and $C_{29}\beta\beta/(\beta\beta+\alpha\alpha)$[40], the hopane parameters $C_{31}\alpha\alpha\alpha 22S/(22S+22R)$ and $Ts/(Ts+Tm)$[40], the methylphenanthrene index (MPI) and the equivalent vitrinite reflectance (Rc)[18] are considered effective maturity indicators.

For the studied shale samples, the CPI values were close to 1.0 (Table 3) and indicative of the mature stage.

Most of the samples yielded high values (>0.4) of the sterane index $C_{29}\beta\beta/(\beta\beta+\alpha\alpha)$, except for samples CY20, CY22, CY27, CY29, and CY39. The end point of sterane index ($C_{29}\alpha\alpha 20S/(20S+20R)$ and $C_{29}\beta\beta/(\beta\beta+\alpha\alpha)$) is 0.52–0.55 and 0.67–0.71, respectively[40]. And the sterane index greater than 0.4 indicate that the organic matter in samples is mature[40]. The values of both of these parameters indicate that the organic matter in the samples obtained from the Chaiye 2 well is mature[40] (Fig. 15).

A mature state was inferred for the organic matter of all samples based on the values of the hopane index $C_{31}22S/(22S+22R)$ and $Ts/(Ts+Tm)$ (Table 3). The hopane indexes indicate that the samples obtained from the Chaiye 2 well are mature[40].

The MPI and the equivalent vitrinite reflectance (Rc, %) are also considered to be highly effective maturity indicators[18]. The MPI and Rc values (Table 3) indicate that the samples obtained from the Chaiye 2 well are mature to highly mature[18].

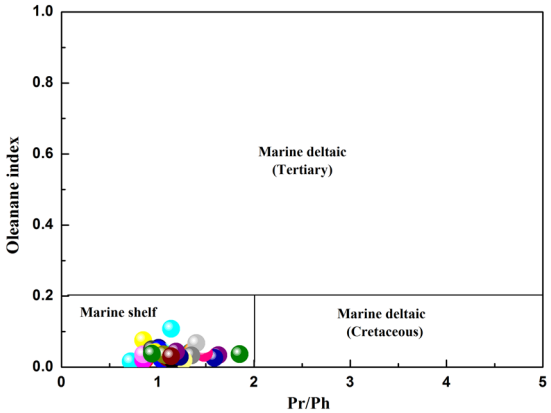

Figure 14. Plot of oleanane index values versus the pristane to phytane (Pr/Ph) ratio, indicating the depositional environment of the shale from the Chaiye 2 well.

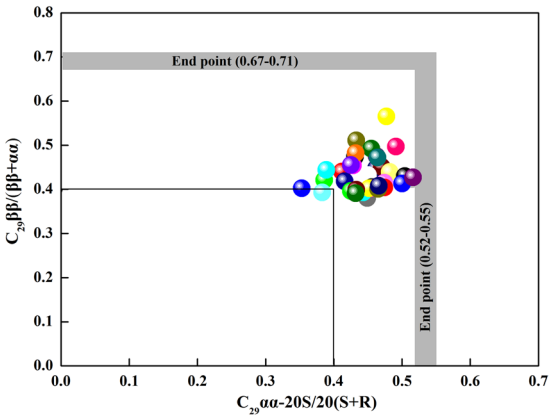

Figure 15. Plot of the sterane index $C_{29}\beta\beta/(\beta\beta+\alpha\alpha)$ versus the sterane index $C_{29}\alpha\alpha 20S/(20S+20R)$, indicating the maturity of the shale samples obtained from the Chaiye 2 well.

Hydrocarbon-generating potential. The gas potential of shale can be evaluated using several standard methods. Zou (2010) and Zumberge (2010) suggested that shale should meet some geochemical criteria be associated a high shale gas potential[41,42]. For example, the TOC content should be greater than 2.0%, the Ro value should be higher than 0.8–1.1%, and the kerogen should be type II or III. In addition, Nie (2009) and Li (2011) argued that TOC contents greater than 1.0% effectively indicate areas of high shale gas potential in China[43,44]. For the shale samples obtained from the Chaiye 2 well, the TOC contents of 75% of the samples were greater than the 2% threshold value (average TOC content: 4.67%), and the TOC contents of 86% of the samples are greater than 1.0% (Table 1). All of the samples reflected a high maturity level that is adequate for the generation of gas. The kerogen type indicates a marine shelf depositional environment and the presence of type III organic matter. Hence, our data and interpretations, as well as the relatively high TOC contents and high maturities of the organic matter in the Chaiye 2 well indicate that the studied shale is suitable for commercial shale gas production.

Additionally, the Tmax and PI values obtained via the Rock-Eval pyrolysis analyses be used to assess the nature of the hydrocarbon products and the degree of maturation in the samples[45]. The relationship between Tmax and PI shows that the shale samples from the Chaiye 2 well in China are in the main stage of hydrocarbon generation (Fig. 16).

Therefore, the organic geochemical characteristics and petrographic results suggest that the shale samples obtained from the Chaiye 2 well have very good gas generation potential.

Methods

Organic geochemical analyses. The shale samples were analyzed using GC-MS and Rock-Eval pyrolysis. The TOC contents of the samples were also determined.

The 36 shale samples were crushed and ground to mesh size smaller than 100, and subjected to Rock-Eval pyrolysis to determine their TOC and volatile hydrocarbon (HC) (S_1), remaining HC generation potential (S_2), production index ($PI = S_1/[S_1+S_2]$), hydrogen index ($HI = S_2/TOC \times 100$), and Tmax value (the temperature corresponding to the maximum value of S_2).

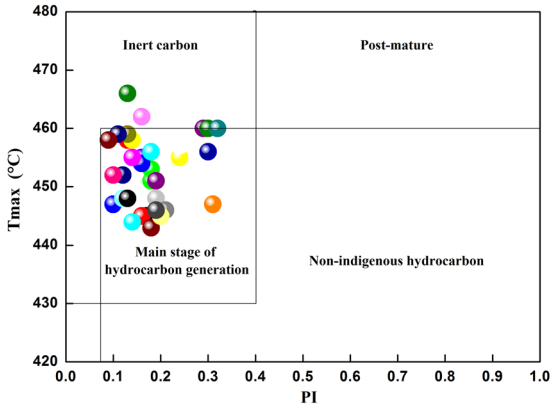

Figure 16. Plot of pyrolysis-based Tmax versus production index (PI) values reflecting the degree of maturation and nature of the hydrocarbon products in the shale samples obtained from the Chaiye 2 well in China.

The Rock-Eval pyrolysis analyses were conducted using a Rock-Eval 6 instrument made in France. The Rock-Eval pyrolysis and TOC analyses were performed on 130 mg of ground material from the shale samples. The ground sample material was heated to 850 °C at a rate of 10 °C/min in a helium atmosphere.

Approximately 150 g of ground material from each shale sample was subjected to Soxhlet extraction using chloroform for 72 h at a constant temperature of 70 °C. The extracts from the shale samples were deasphalted by precipitation with n-hexane and filtration. The deasphalted maltenes were fractionated into saturates and aromatics via column chromatography using activated silica gel and aluminum oxide (v:v = 3:1) with n-hexane and methylene chloride, respectively[46]. Saturates and aromatics were then analyzed using GC-MS.

The GC-MS analyses were performed using an Agilent 6890N GC interfaced with a 5973 MS. An Agilent HP-5 column (30 m × 0.25 mm i.d., 0.25 μm film thickness) was used. The injection temperature was 70 °C (2 min hold), and the temperature program was 4 °C/min from 80 °C to 290 °C (30 min hold). The flow rate of the carrier gas (He) was 1.1 mL/min, and the pressure was 2.4 kPa. The sample injection volume was 1.0 L, and the split ratio was 10:1. Electron impact (EI) ionization at 70 eV was used for the ion source. The temperatures of the transfer line and ion source were 280 °C and 230 °C, respectively. The parent ion was m/z 285, the activating voltage was 1.5 V, and the scanning range was from m/z 35 to 600.

Petrographic analyses. The vitrinite reflectance values were measured in random mode and reported in Ro (%). The samples were mounted in resin and were then ground into pellets and polished using alumina–ethanol slurry. The measurements were performed under oil immersion at a wavelength of 546 mm using a Leitz Orthoplan/MPV-SP photometer microscope system.

Petrographic analyses were performed on the polished shale samples under reflected white light following conventional methods using the Leitz Orthoplan/MPV-SP photometer microscope system. Each sample was measured at least 500 times.

Conclusions

The geochemical and petrographic analyses of the Carboniferous shale penetrated by the Chaiye 2 well in the Qaidam Basin suggest the following conclusions. The organic matter within these rocks originated in a marine shelf depositional environment. This conclusion is supported by various geochemical parameters, such as Pr/Ph; Pr/n-C_{17}, Ph/n-C_{18}, C_{27}, C_{28} and C_{29} αα steranes, C_{29}/C_{27} regular steranes, the gammacerane index, the oleanane index, and the DBT/P ratio of the aromatics. The high TOC contents of these rocks include large amounts of vitrinite and sapropelinite, and this organic matter is characterized as a highly mature type III kerogen. These conclusions are supported by the values of various geochemical parameters, such as TOC, KTI, HI, Ro, Tmax, the CPI of the n-alkanes, the sterane parameters C_{29}αα20S/(20S + 20R) and C_{29}ββ/(ββ + αα), the hopane parameters C_{31}22S/(22S + 22R) and Ts/(Ts + Tm), the MPI and the Rc of the aromatics as well as the molecular composition of the hydrocarbons. The Carboniferous shale penetrated by the Chaiye 2 well has very good gas generation potential, as indicated by the large amounts of highly mature type III organic matter in the shale (the TOC contents of 86% of the samples exceeded 1.0%), which originated in a marine shelf depositional environment.

References

1. Hill, D. G. & Nelson, C. R. Reservoir properties of the Upper Cretaceous Lewis Shale, a new natural gas play in the San Juan Basin. *AAPG Bulletin* **84**, 1240 (2000).
2. Li, J. X., Lv, Z. G., Dong, D. Y. & Cheng, K. M. North American shale gas resources forming geological conditions. *Natural Gas Industry* **29**, 27–32 (2009).
3. Soroush, H., Rasouli, V. & Tokhmechi, B. A data processing algorithm proposed for identification of breakout zones in tight formations: A case study in Barnett gas shale. *Journal of Petroleum Science and Engineering* **74**, 154–162 (2010).
4. Zhang, J. C., Niu, H. K., Xu, B., Jiang, S. L. & Zhang, P. X. Geological condition of shale gas accumulation in Sichuan Basin. *Natural Gas Industry* **28**, 151–156 (2008).

5. Dang, W. Z. *et al*. Main-controlling geological factors of gas-bearing property of continental shale gas: a case study of Member 3rd of Shahejie Formation in western Liaohe sag. *Acta Petrolei Sinica* **36**, 1516–1530 (2015).
6. Curtis, J. B. Fractured shale gas systems. *AAPG Bulletin* **86**, 1921–1938 (2002).
7. Niu, H. K., Tang, X. & Bian, R. K. Controlling factors for shale gas accumulation and prediction of potential development area in shale gas reservoir of south China. *Acta Petrolei Sinica* **30**, 484–491 (2009).
8. Ding, W. L., Li, C., Su, A. G. & He, Z. H. Study on the comprehensive geochemical cross section of Mesozoic marine source rocks and prediction of favorable hydrocarbon generation area in Qiangtan basin, Tibeta. *Acta Petrologica Sinica* **27**, 878–896 (2011).
9. Dong, D. Y., Zhou, C. N., Yang, H., Wang, Y. M. & Li, X. L. China shale gas exploration and development progress and development prospect. *Acta Petrolei Sinica* **33**, 107–114 (2012).
10. David, W. H. *et al*. Early Triassic (early Olenekian) life in the interior of East Gondwana: mixed marine–terrestrial biota from the Kockatea Shale Western Australia. *Palaeogeography, Palaeoclimatology, Palaeoecology* **417**, 511–533 (2015).
11. Guo, S. B., Fu, J. J., Gao, D., Li, H. Y. & Huang, J. Y. Research status and prospects for marine-continental shale gases in China. *Petroleum Geology & Experiment* **37**, 535–540 (2015).
12. Peng, D. H., Chen, Q. L. & Chen, Y. B. Evaluation of geologic features and potential petroleum pesource in Delingha depression of Qaidam Basin. *China Petroleum Exploration* **6**, 45–50+130 (2006).
13. Chen, Y. B. & Hu, Y. Wang Y.q. Evaluation on Carboniferous source rock in Delingha Depression of Qaidam Basin. *Special Oil & Gas Reservoirs* **21**, 43–48 (2014).
14. Lin, C. G. Re-recognition of Carboniferous and Jurassic distribution of DLHA depression, eastern Qaidam Basin. *Geological Bulletin of China* **35**, 293–301 (2016).
15. Cao, J. *et al*. Geochemical characreristics and genesis of shale gas for Carboniferous marinecontinental transitional facies coal measure strata in Eastern Qaidam Basin. *Earth Science Frontiers (China University of Geosciences(Beijing); Peking University)* **23**, 158–166 (2016).
16. Ma, Y. S. *et al*. The Progress of Carboniferous Oil and Gas Investigation and Assessment in Qaidam Basin. *Acta Geoscientica Sinica* **33**, 135–144 (2012).
17. Liu, C. L. *et al*. Evidence for the carboniferous hydrocarbon generation in Qaidam Basin. *Acta Petrolei Sinica* **33**, 925–931 (2012).
18. Radke, M. Application of aromatic compounds as maturity indicators in source rocks and crude oils. *Marine and Petroleum Geology* **5**, 224–236 (1988).
19. Corte, J. E. *et al*. Molecular organic geochemistry of the Apiay field in the Llanos basin, Colombia. *Journal of South American Earth Sciences* **47**, 166–178 (2013).
20. Mohammed, H. H., Abdulghani, F. A. & Wan, H. A. Organic geochemical and petrographic characteristics of the Miocene Saliforganic-rich shales in the Tihama Basin, Red Sea of Yemen: Implicationsfor paleoenvironmental conditions and oil-generation potential. *International Journal of Coal Geology* **154-155**, 193–204 (2016).
21. Liu, H. H. *et al*. Organic geochemical characteristics of Carboniferous-Permian mud shale from Huainan area. *Journal of Central South University (Science and Technology)* **47**, 2109–2118 (2016).
22. Mohammed, H. H., Wan, H. A. & Mohamed, R. S. Geochemical and petrographic characterization of organic matter in the UpperJurassic Madbi shale succession (Masila Basin, Yemen): Origin, type andpreservation. *Organic Geochemistry* **49**, 18–29 (2012).
23. Peters, K.E. & Cassa, M.R. Applied source rock geochemistry. In: Magoon, L.B.,Dow, W.G. (Eds.), The Petroleum System – From Source to Trap. AmericanAssociation of Petroleum Geologists Memoir **60**, 93–120(1994).
24. Duan, Y. & Ma, L. H. Lipid geochemistry in a sediment core from Ruoergai Marshdeposit (Eastern Qinghai-Tibet plateau, China). *Organic Geochemistry* **32**, 1429–1442 (2001).
25. Duan, Y. Organic geochemistry of recent marine sediments from the Nansha Sea, China. *Organic Geochemistry* **31**, 159–167 (2000).
26. Wang, Y. P., Zhang, F., Zou, Y. R., Zhan, Z. W. & Peng, P. A. Chemometrics reveals oil sources in the Fangzheng Fault Depression, NE China. *Organic Geochemistry* **102**, 11–13 (2016).
27. Sun, X., Zhang, T. W., Sun, Y. G., Millikena, K. L. & Sun, D. Y. Geochemical evidence of organic matter source input and depositional environments in the lower and upper Eagle Ford Formation, south Texas. *Organic Geochemistry* **98**, 66–81 (2016).
28. Mohamed, M. E., Fatma, M. H. & Naglaa, S. M. Biomarker characteristics of crude oils from Ashrafi and GH oilfields in the Gulf of Suez, Egypt: An implication to source input and paleoenvironmental assessments. *Egyptian Journal of Petroleum* **23**, 455–459 (2014).
29. Armelle, R. *et al*. Environmental change during the Early Cretaceous in the Purbeck-type Durlston Bay section (Dorset, Southern England): A biomarker approach. *Organic Geochemistry* **38**, 1804–1823 (2007).
30. Karwan, A. M., Mark, A. S., Jonathan, S. W., Fivos, S. & Piotr, K. Organic geochemical characteristics of black shales across the OrdovicianeSilurian boundary in the Holy Cross Mountains, central Poland. *Marine and Petroleum Geology* **66**, 1042–1055 (2015).
31. Mohammed, H. H., Wan, H. A., Mohamed, R. S. & Gamal, A. A. Geochemistry and organic petrology study of Kimmeridgian organicrich shales in the Marib-Shabowah Basin, Yemen: Origin and implication for depositional environments and oil-generation potential. *Marine and Petroleum Geology* **50**, 185–201 (2014).
32. Dutta, S., Bhattacharya, S. & Raju, S. V. Biomarker signatures from Neoproterozoic–Early Cambrian oil, western India. *Organic Geochemistry* **56**, 68–80 (2013).
33. Wang, L., Song, Z. G., Cao, X. X. & Li, Y. Compound-specific carbon isotope study on the hydrocarbon biomarkers in lacustrine source rocks from Songliao Basin. *Organic Geochemistry* **87**, 68–77 (2015).
34. Chang, X. C., Wang, T. G., Li, Q. M., Cheng, B. & Tao, X. W. Geochemistry and possible origin of petroleum in Palaeozoic reservoirs from Halahatang Depression. *Journal of Asian Earth Sciences* **74**, 129–141 (2013).
35. Holba, A. G. *et al*. Application of tetracyclic polyprenoids as indicators of input from fresh-brackish water environments. *Organic Geochemistry* **34**, 441–469 (2003).
36. Wan, L. K., Liu, J. G., Mao, F. J., Lv, M. S. & Liu, B. The petroleum geochemistry of the Termit Basin, Eastern Niger. *Marine and Petroleum Geology* **51**, 167–183 (2014).
37. Neeraj, M. Tertiary oils from Upper Assam Basin, India: A geochemical study using terrigenous biomarkers. *Organic Geochemistry* **76**, 9–25 (2014).
38. Alberdi, M. & Lopez, L. Biomarkers 18(H)-oleanane: a geochemical tool to assess Venezuelan petroleum systems. *Journal of South American Earth Sciences* **13**, 751–759 (2000).
39. Tao, S., Tang, D. Z., Xu, H., Liang, J. L. & Shi, X. F. Organic geochemistry and elements distribution in Dahuangshan oil shale, southern Junggar Basin: Origin of organic matter and depositional environment. *International Journal of Coal Geology* **115**, 41–51 (2013).
40. Chen, Z. H. *et al*. Oil origin and accumulation in the Paleozoic Chepaizi–Xinguang field, Junggar Basin, China. *Journal of Asian Earth Sciences* **115**, 1–15 (2016).
41. Zou, C. N. *et al*. Geological characteristics and resource potential of shale gas in China. *Petroleum Exploration and Development* **37**, 641–653 (2010).
42. Zumberge j., Kevin Ferworn K. & Brown S. Isotopic reversal ('rollover') in shale gases produced from the Mississippian Barnett and Fayetteville formations. Marine and Petroleum Geology **31**, 43–52(2012).
43. Nie, H. K., Tang, X. & Bian, R. K. Controlling factors for shale gas accumulation and prediction of potential development area in shale gas reservoir of South China. *Acta Petrolei Sinica* **30**, 484–491 (2009).
44. Li, Y. J., Liu, H., Liu, J. X., Cao, L. C. & Jia, X. C. Gelolgical regional selection and an evaluation method of resource potential of shale gas. *Journal of Southwest Petroleum University: Science & Technology Edition* **33**, 28–34 (2011).

45. Mohammed, H. H. & Wan, H. A. Organic geochemical characteristics and oil generating potential of the Upper Jurassic Safer shale sediments in the Marib-Shabowah Basin, western Yemen. *Organic Geochemistry* **54**, 115–124 (2013).
46. Sun, M. Z. *et al*. Geochemical Characteristics of Bitumen "A" in Marine Carbonate Rock from the Tarim Basin. Rock and Mineral. *Analysis* **30**, 623–630 (2011).

Acknowledgements

This study was supported by the National Natural Science Foundation of China (grant no. 41603014) and by a Key Laboratory Project of Gansu Province (grant no. 1309RTSA041). All the experiments were performed at the Public Technical Service Center of the Lanzhou Center for Oil and Gas Resources, Institute of Geology and Geophysics, Chinese Academy of Sciences. We thank American Journal Experts (AJE) for providing English language editing.

Author Contributions

G.-C.W., M.-Z.S. and S.-F.G. collected the samples. M.-Z.S. and L.T. prepared the samples. G.-C.W. conceived the project and analyzed the samples. G.-C.W. interpreted the data. After discussions with M.-Z.S., G.-C.W. wrote the paper with S.-F.G. and L.T. All authors reviewed the manuscript.

Additional Information

Supplementary information accompanies this paper at https://doi.org/10.1038/s41598-018-25051-1.

Competing Interests: The authors declare no competing interests.

Publisher's note: Springer Nature remains neutral with regard to jurisdictional claims in published maps and institutional affiliations.